RSC Advances

ROYAL SOCIETY OF CHEMISTRY

www.rsc.org/advances

DFT Study on the CuBr-Catalyzed Synthesis of Highly Substituted Furans: Effects of Solvent DMF, Substrate MeOH, Trace H_2O and Metallic Valence State of Cu

Binfang Yuan, Rongxing He, Wei Shen, Weixia Hu, Ming Li*

Key Laboratory of Luminescence and Real-Time Analytical chemistry (Southwest University), Ministry of Education, College of Chemistry and Chemical Engineering, Southwest University, Chongqing 400715, China

* To whom correspondence should be addressed. E-mail: liming@swu.edu.cn

Abstract: The CuBr-catalyzed 2-(1-alkynyl)-2-alken-1-ones is selected as a research system to explore the effects of solvent DMF, substrate MeOH, trace H_2O and valence state of Cu on the synthesis of highly substituted furans using the BHandHLYP density functional. Our calculations suggest that DMF, MeOH and H_2O can be used as hydrogen-bond acceptors to accelerate the intermolecular nucleophilic addition. More importantly, they play the role of proton shuttles to assist H migration significantly by reducing the free energy barrier of H-transfer process. Due to the participation of DMF, MeOH or H_2O, the rate-determining step is changed from the H-transfer process (96.0 kJ/mol) to the intramolecular cyclization step (57.6 kJ/mol). In addition, calculated results also discover that the yield can be further improved when CuBr is replaced by $CuBr_2$. In short, the present study can provide an insight into the metal-catalyzed reactions involving H-transfer process and a guideline used to the design of new catalysts for the metal-catalyzed reaction applications.

Introduction

Highly substituted furans not only can be used as key structural units in many natural products and pharmaceuticals[1], but also act as important precursors in the synthesis of acyclic, carbocyclic, and heterocyclic compounds[2]. For these reasons, they have played a crucial role in organic synthesis chemistry for more than one hundred years. As we know, the cyclization of 1,4-diketones mediated by strong mineral acids was considered to be the classical approach for the synthesis of furans in the past decades, and this synthesis measure was commonly referred to as the Paal-Knorr reaction.[3] However, it is restricted to a large extent due to the limited availability of different 1,4-diketones and the requirement for a strong acid. In recent years, the transition metals have been employed as catalysts to catalyze the synthesis of substituted furans in good results under mild reaction conditions.[1d, 4] Liang and co-workers reported that the highly substituted furans are prepared from 1-oxiranyl-2-alkynyl esters and a range of nucleophiles including alcohols, furans and pyrroles under gold catalysis.[5] Larock et al. discovered a new catalytic approach to synthesize highly substituted furans from 2-(1-alkynyl)-2-alken-1-ones with various nucleophiles under very mild reaction with $AuCl_3$ as an effective catalyst.[6] Gevorgyan et al. demonstrated that the Au(III)-catalyzed 1,2-iodine, -bromine, and -chlorine migration in haloallenyl ketones lead to 3-halofurans via a halirenium intermediate in good to excellent yields.[7] A convenient one-pot Cu(I)-catalyzed strategy for regioselective synthesis of trisubstituted furan derivatives has been developed by Cao et al.[8] This process has opened a new synthetic route to a variety of α-carbonyl furans in good yields using air as the oxidant affording furans. Thus, the application of transition metals continues to attract the interest of many synthetic chemists for the synthesis of highly substituted furans. In addition, solvents also have some significant effect on the synthesis of highly substituted furans.[4a, 9] Pale et al. declared that dichloromethane and methanol are combined as an

appropriate mixed solvent to effectively promote the silver(I)-catalyzed synthesis of Furans.[10] More importantly, Yamamoto and co-workers found that solvent DMF not only provides favorable catalytic medium for the synthesis of highly substituted furans from 2-(1-Alkynyl)-2-alken-1-ones with Cu(I) salts as catalysts, but also acts as a cocatalyst to directly participate in the reaction.[11] The properties of solvent-assisted catalytic reaction also were proposed by Yamamoto et al. in the synthesis of cyclic alkenyl ethers via intramolecular cyclization of o-alkynylbenzaldehydes.[12] According to the above discussion, both of the metal catalysts and solvents have some important roles in the synthesis of highly substituted furans. These roles are worthy of in-depth study by the experimental and theoretical methods.

Scheme 1. The CuBr-catalyzed synthesis of highly substituted furans from 2-(1-alkynyl)-2-alken-1-ones with nucleophile MeOH (excess) in DMF solvent (no dry).

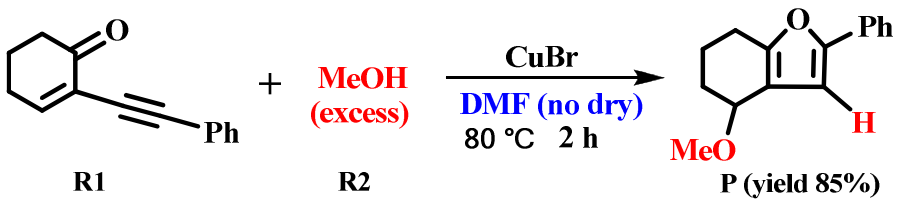

In our study, we choose the CuBr-catalyzed synthesis of highly substituted furans from 2-(1-alkynyl)-2-alken-1-ones with nucleophile MeOH (excess) in DMF medium as a simple research system[11] to explore the effects of metal catalyst CuBr, solvent DMF, excess substrate MeOH and trace amounts of H_2O (presented in the solvent), as shown in Scheme 1. Besides, the calculations also discover that the high valence state of copper is stronger than its low valence state in catalytic ability for the present catalytic reaction.

2 Computation Methods

All calculations are performed with Gaussian 09 suite of programs.[13] All the geometries of the species, intermediates and transition states, are fully optimized by using the BHandHLYP method of

density functional theory (DFT)[14], which is based on the Becke's half-and-half method and the gradient-corrected correlation functional of Lee and co-workers.[15] This computational method has been successfully applied in the mechanistic studies of transition-metal- or non-transition-metal-catalyzed reactions.[16] For C, O, Br, and H elements, the double-ζ basis set (6-31G*)[17] is employed, while Cu is described by the effective core potential double-ζ basis set (LanL2DZ)[18]. This combination of basis sets (6-31G* and LanL2DZ) has also been proven to be reliable in numerous theoretical simulations of mechanisms of metal-catalyzed reactions.[16d, 19] Frequency calculations are carried out at the same level to identify each stationary point to be either a minimum or a transition structure. When the animation of transition state's vibrations cannot easily confirm the reliability of transition states, the intrinsic reaction coordinate (IRC)[20] calculations will be conducted to unambiguously identify the transition states, which are connected with the reactants and the products. All the key of IRC calculations are described in the Supporting Information. The charge decomposition analysis (CDA) and the construction of orbital interaction diagrams are performed by using AOMix-CDA[21] to show the difference of CuBr and $CuBr_2$ in catalytic capability. According to the optimal structures obtained, solvent effect of DMF (ε =37.22) is taken into account with a self-consistent reaction field (SCRF) method[22] based on the polarizable continuum model (PCM)[23] at the BHandHLYP/6-311++G** (LanL2DZ for Cu) level. All the discussed energies are relative Gibbs free energies (ΔG_{rel}) in DMF solvent unless special emphasis.

3 Results and Discussion

3.1 Functions of DMF, MeOH and H_2O. In this section, we first study on the mechanism of CuBr-catalyzed synthesis of highly substituted furans from 2-(1-alkynyl)-2-alken-1-ones with nucleophile MeOH (excess) in DMF medium, and then a detailed discussion about the cocatalyst-assisted processes is presented to understand the roles of DMF, MeOH and H_2O in the

rate acceleration of this reaction.

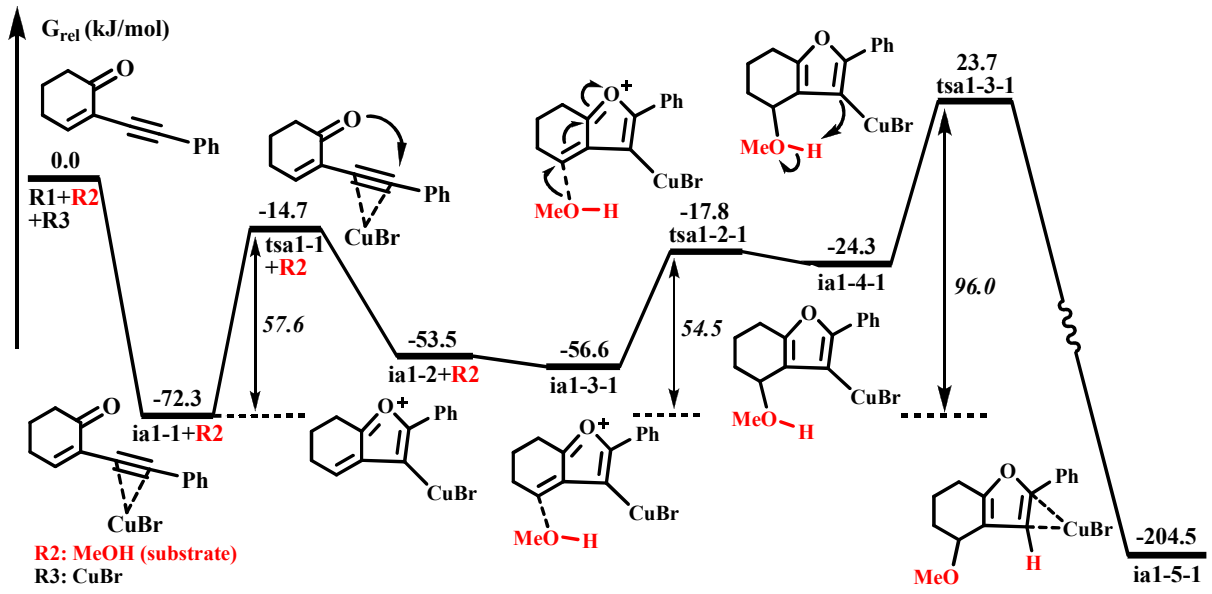

Figure 1. DFT-computed energy profile for the CuBr-catalyzed synthesis of highly substituted furans without the participation of cocatalyst.

Mechanism of Synthesis of Highly Substituted Furans in DMF Medium. The DFT-computed energy profile for the synthesis of highly substituted furans is given in Figure 1, and the optimized structures along the reaction path are showed in Figure 2. The catalytic reaction starts with coordination of CuBr to the C1-C2 triple bond of 2-(1-alkynyl)-2-alken-1-ones (R1) to form the complex ia1-1. In principle, there are four kinds of models for the coordination of CuBr with 2-(1-alkynyl)-2-alken-1-ones (R1), CuBr/C1-C2 triple bond, CuBr/O1, CuBr/(C1-C2 and O1) and CuBr/C3-C4 double bond, and these coordination forms produce complexes ia1-1, ib1-1, ic1-1 and id1-1, respectively, as shown in Figure S1 of the Supporting Information. Based on our calculated results, we find that the first coordination mode, CuBr/C1-C2 triple bond, is one feasible strategy compared with other three coordination cases (calculations related to the unfavorable coordination forms are described in Figures S3-S7 of the Supporting Information). In this coordinated strategy, the resonance-stabilized oxonium ion ia1-2 is formed firstly by the nucleophilic attack of carbonyl

oxygen on the copper-coordinated alkynes (from ia1-1 to ia1-2 though tsa1-1, see Figure 1), and then ia2-1 is trapped by a MeOH to form the final products P (highly substituted furans).

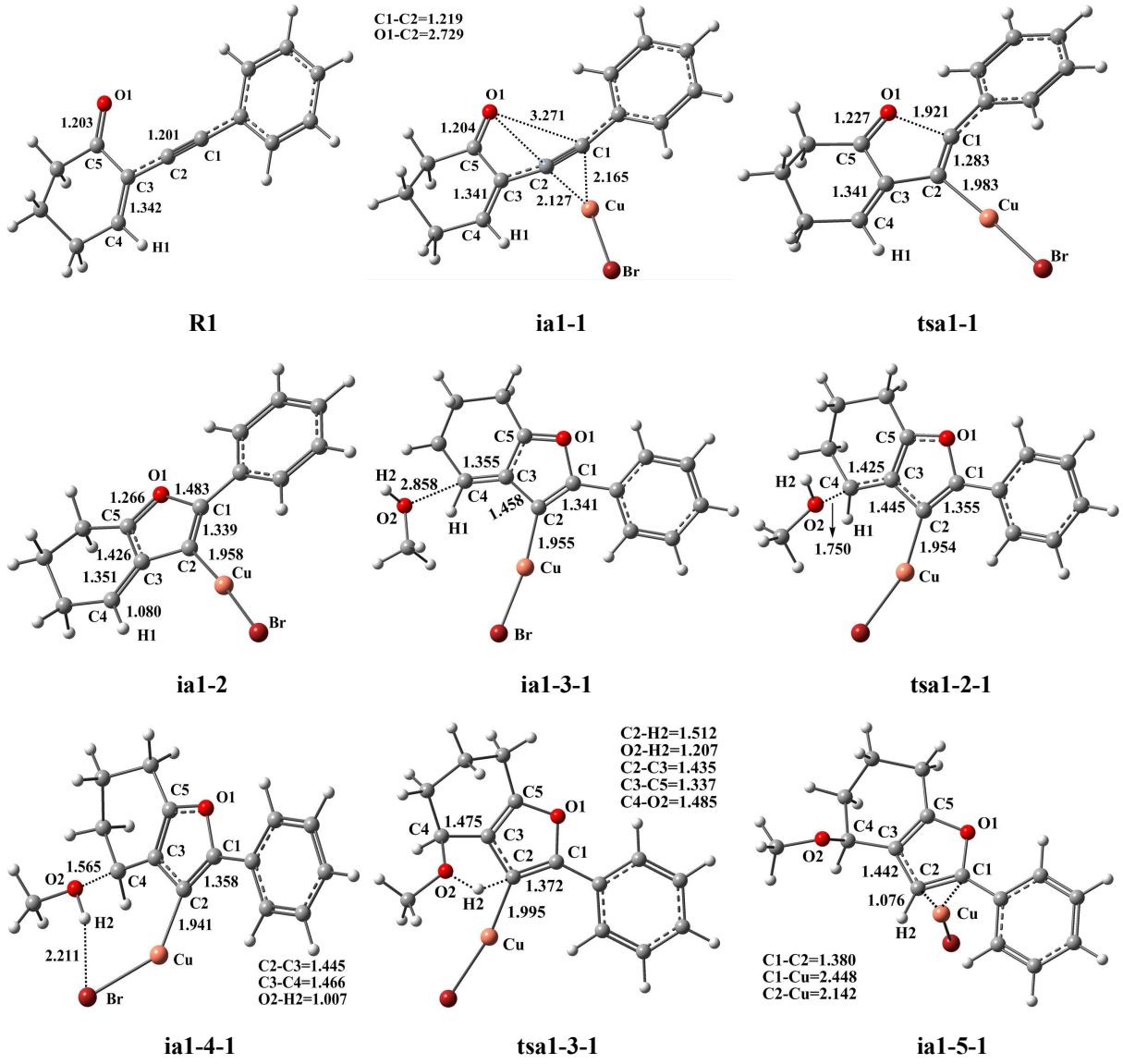

Figure 2. Optimized structures for the CuBr-catalyzed synthesis of highly substituted furans without the participation of cocatalyst DMF, MeOH and H_2O (selected structural parameters are listed (bond lengths in Å)).

This mechanism has already been reported by Yamamoto, Abbiati and Belmont.[11, 12, 24] In short, the coordination of CuBr with C1-C2 is the most favorable for the synthesis of highly substituted furans. Besides, although the formation of these coordination complexes is very exothermic, the energies generated from coordination process would be quickly released into the environments under

non-adiabatic conditions and could not contribute to the following procedure. This similar fact has been supported by Zhang's group.[25] Therefore, the reactants need to be heated at 80℃ in order to get the final products P.

Figure 1 shows that the formation of complex ia1-1 is exergonic by 72.3 kJ/mol in DMF solvent. In ia1-1, the C1-C2 bond has lost a little of its triple-bond characters, and is now 1.219 Å (1.201 in R1). This means that the C1-C2 triple bond has been activated. In the further reaction, the carbonyl oxygen O1, which acts as an electron donor, attacks the activated C1-C2 triple bond to lead to an organocopper intermediate ia1-2 via a transition state tsa1-1. In ia1-2, the C3-C4 bond is extended from 1.341 (in ia1-1) to 1.351 Å due to the formation of C1-O1 bond (1.483 Å). Obviously, the double-bond energy of C3-C4 is weakened, which is favorable for the subsequent reactions. In the intermolecular nucleophilic addition reaction, ia1-2 captures a MeOH molecule by the interaction of C4 and O2 (C4-O2=1.715 Å), leading to a more stable intermediate ia1-3-1. As the reaction proceeds, the methanol hydroxyl oxygen O2 as a nucleophile attacks on C4 of C3-C4 double bond to form a new complex ia1-4-1 via a transition state tsa1-2-1. In ia1-4-1, the C3-C4 bond is extended to 1.466 Å with forming the C4-O2 bond (1.565 Å). It is worth noting that the Mulliken charges for C2, C3, and H2 are -0.180, -0.055, and 0.517 in ia1-4-1, respectively, which means that H2 is more easily transferred to C2 via a 1,4-H shift process (the other H2-migration process is described in Figure S9 of the Supporting Information). In the 1,4-H shift process, ia1-4-1 goes through a transition state tsa1-3-1 to form a stable complex ia1-5-1. At last, the ia1-5-1 decomposes into the furans P with the regeneration of metal catalyst CuBr. In addition, H2 is likely to be migrated to Br of CuBr. We try our best to find this H-transfer case, but we failed.

As illustrated in Figure 1, DFT-computed energy profile of the CuBr-catalyzed synthesis of highly substituted furans includes three elementary processes, an intramolecular cyclization, an

intermolecular addition and a 1,4 H-shift process. Their required energy barriers are 57.6, 54.5 and 96.0 kJ/mol, respectively. Obviously, 1,4 H-shift process is the rate-limiting step of the whole catalytic reaction. The rate-limiting energy barrier is 96.0 kJ/mol, which is unfavorable for the synthesis of highly substituted furans. In the following sections, we turn our attention to the effects of DMF, MeOH and H_2O on the catalytic reactions.

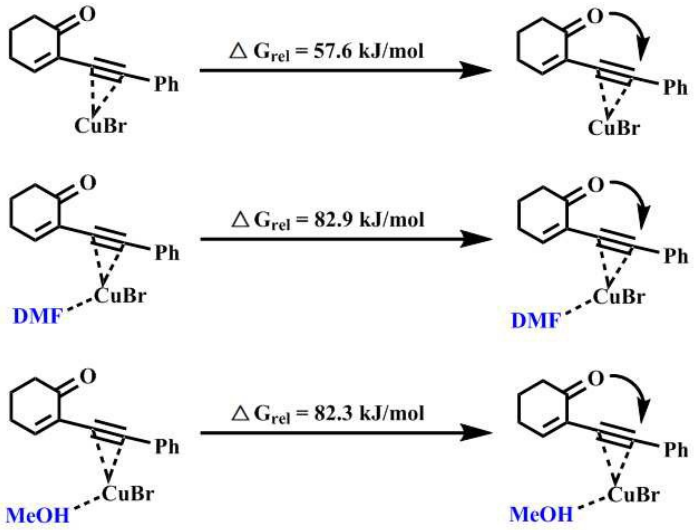

Scheme 2. Comparison of the activation free energies for intramolecular cyclization reaction without and with DMF or MeOH as a ligand.

Effects of DMF and MeOH on the Intramolecular Cyclization. Theoretically, DMF and MeOH can directly affect all steps of Figure 1. Here**,** we firstly discuss the influence of DMF and MeOH on the intramolecular cyclization. The molecule of DMF or MeOH as a ligand coordinates with the metal catalyst CuBr, but the participation of DMF and MeOH do not alter the reaction mechanism of intramolecular cyclization process, as shown in Scheme 2. In the present situations, the activation free energies of CuBr(DMF)- and CuBr(MeOH)-catalyzed cyclization reaction are 82.9 and 82.3 kJ/mol, respectively, which are 25.3 and 24.7 kJ/mol higher than that of the case without DMF or

MeOH as the ligand. This means that the effects of DMF and MeOH on the intramolecular cyclization process are negative.

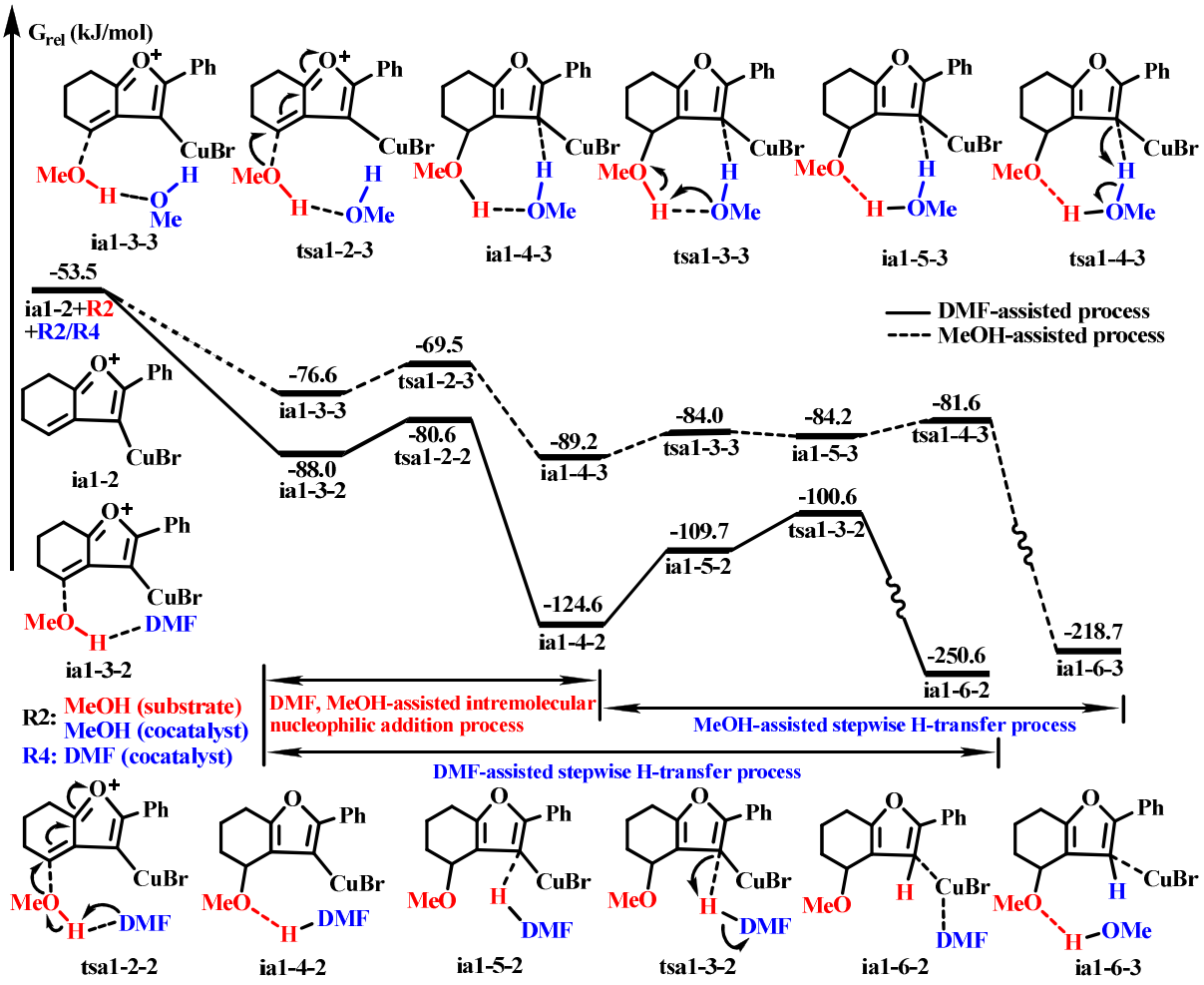

Figure 3. DFT-computed energy profiles of the DMF- and MeOH-assisted processes in the CuBr-catalyzed synthesis of highly substituted furans.

Effects of DMF and MeOH on the Intermolecular Addition. As indicated in Figure 3, ia1-2 can capture a MeOH molecule (as substrate) and a DMF molecule, or seize two MeOH molecules (one as a substrate, and another as a cocatalyst) via a weak interaction between C4 and O2 and a hydrogen-bond of O2-H2···O3 (O4), leading to the generation of stable complexes ia1-3-2 and ia1-3-3 with releasing energies of 34.5 and 23.1 kJ/mol, respectively. The geometrical structures of

ia1-3-2 and ia1-3-3 are described in Figure 4. Subsequently, a molecule of DMF or MeOH acts as the cocatalyst (Lewis base) to facilitate the intermolecular nucleophilic addition between O2 and C4 through a transition state tsa1-2-2 or tsa1-2-3, forming an intermediate ia1-4-2 or ia1-4-3. Noteworthy, the reaction mechanisms of DMF- and MeOH-assisted intermolecular addition processes are different. The DMF-assisted process includes the formation of C4-O2 bond and the H2 migration from O2 to O3, which is a concerted reaction. However, H2-transfer does not occur in the MeOH-assisted process (see tsa1-2-2 or tsa1-2-3 in Figure 4). In short, our present calculations reveal that DMF and MeOH can be used as hydrogen-bond acceptors to weaken O2-H2 bond via the hydrogen-bond of O2-H2···O3 (O4), aiming to promote the addition reaction of O2 and C4. The energy barrier of intermolecular addition reaction with the assistance of DMF and MeOH is 7.4 and 7.1 kJ/mol, respectively. This indicates that the addition reaction is easy to be performed.

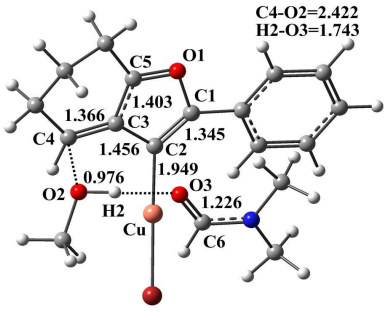

ia1-3-2

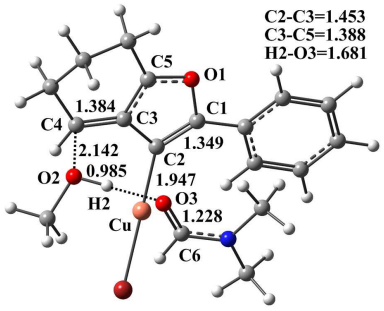

tsa1-2-2

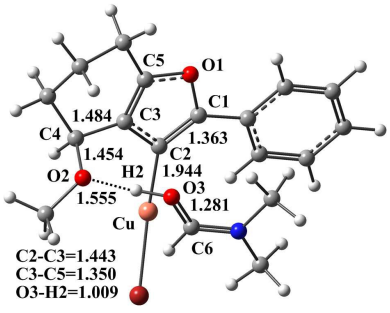

ia1-4-2

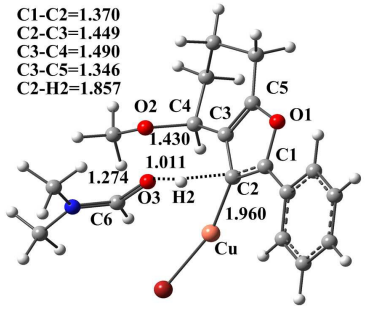

ia1-5-2

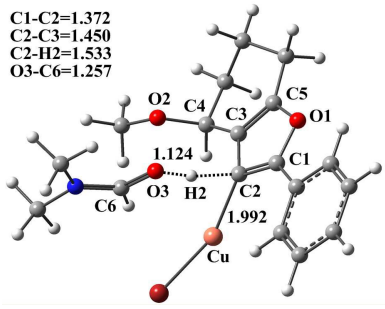

tsa1-3-2

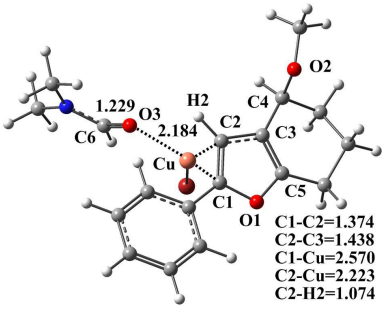

ia1-6-2

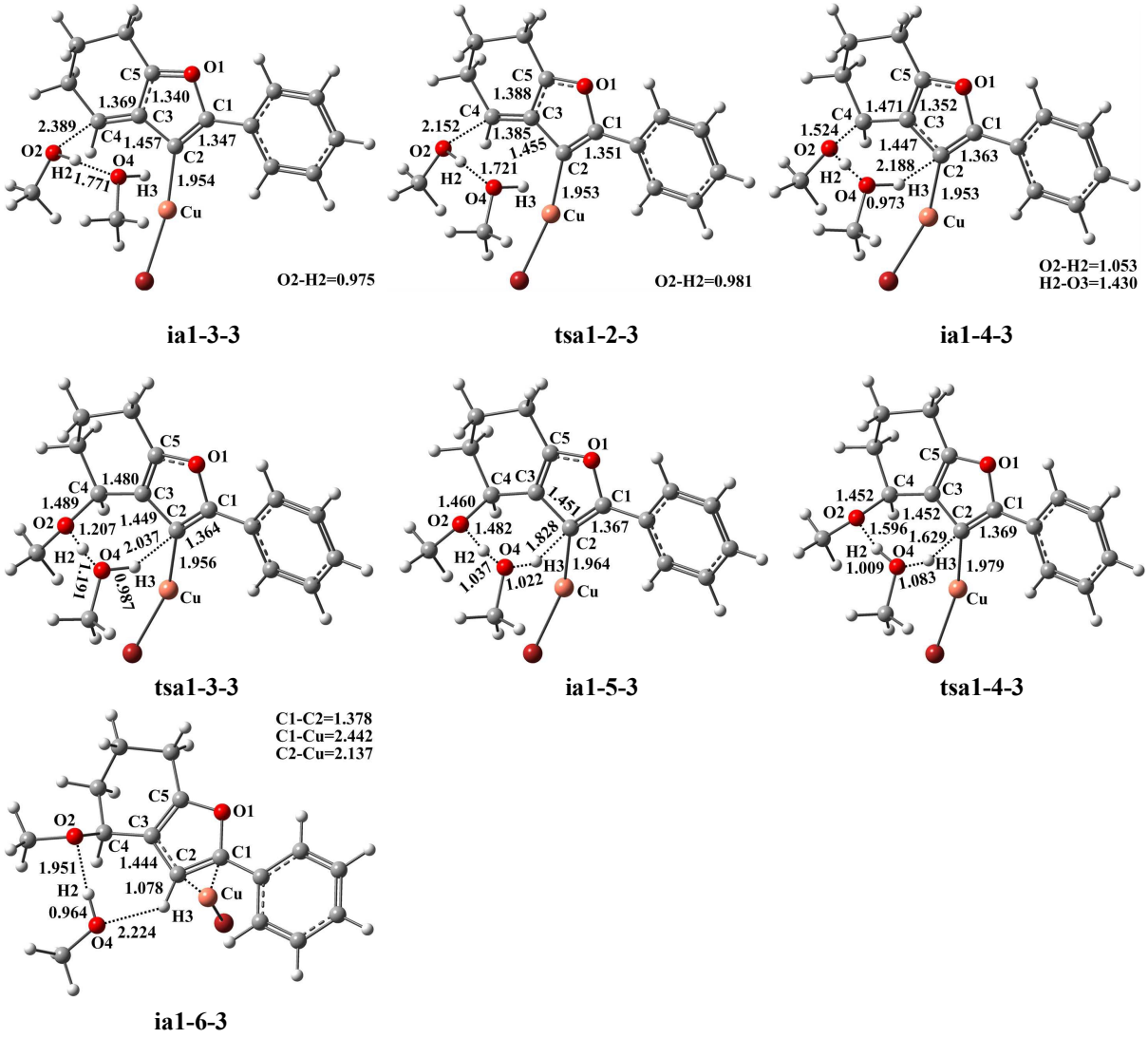

Figure 4. Optimized structures of the DMF- and MeOH-assisted intermolecular addition and stepwise H-transfer processes in the CuBr-catalyzed synthesis of highly substituted furans (selected structural parameters are listed (bond lengths in Å)).

Effects of DMF and MeOH on the H-transfer Process. In the participation of DMF and MeOH, the 1,4 H-shift process (see Figure 1) is changed to a cocatalyst (DMF or MeOH)-assisted stepwise H-transfer process including a protonation of cocatalyst and a deprotonation of cocatalyst-H^+, which is quite similar to the proton-transfer process in proton-transport catalysis[26] and many enzyme-catalyzed reactions[27]. The computed energy profiles of DMF- and MeOH-assisted H-transfer are illustrated in Figure 3, and related geometric structures are collected in Figure 4. In

the protonation of cocatalyst, a molecule of DMF or MeOH as an assisted catalyst seizes H2 from MeOH (as substrate) via a transition state tsa1-2-2 or tsa1-3-3 to form an intermediate ia1-4-2 or ia1-5-3, respectively. It is worth noting that the protonation of DMF process involves the nucleophilic addition between C4 and O2 and the H2 migration from O2 to O3 (from DMF), but only the H2-transfer from O2 to O4 (from MeOH) is included in the protonation of MeOH process. Therefore, DMF- and MeOH-assisted strategies have different reaction mechanisms for the protonation of cocatalyst process. The following reaction is the deprotonation of cocatalyst-H^+. In the deprotonation of DMF-H^+, ia1-4-2 is isomerize to an unstable intermediate ia1-5-2, and then ia1-5-2 passes through a transition state tsa1-3-2 to form a more stable intermediate ia1-6-2 with H2 (form DMF-H^+) migration from O3 to C2. Finally, ia1-6-2 decomposes into the products P and DMF with regenerating the metal catalyst CuBr. Similar to the deprotonation of DMF-H^+, a proton (form MeOH-H^+) is migrated through a little energy barrier of tsa1-4-3 (2.6 kJ/mol) from ia1-5-3 to ia1-6-3 in the deprotonation of MeOH-H^+. However, the geometric structure of tsa1-4-3 displays that the proton transferred is H3 (form cocatalyst MeOH), but not H2 (form substrate MeOH), which means that H3 is transferred to C2 from O4. At last, ia1-6-3 releases the products P, MeOH (as cocatalyst) and the metal catalyst CuBr to complete the catalytic cycle. Briefly, in the present cocatayst-assisted H-shift strategy, DMF or MeOH plays a role of proton shuttle to help a proton transfer from MeOH to C2 of R1. In the DMF- and MeOH-assisted H-transfer reactions, the deprotonation of cocatalyst-H^+ step has a high energy barrier compared with the protonation of cocatalyst step (7.4 vs 24 and 5.2 vs 7.2, see Figure 3). The higher energy barriers are 24.0 and 7.6 kJ/mol for the DMF- and MeOH-assisted H-shift process, which is 72.0 and 88.4 kJ/mol lower than that of 1,4-H transfer process (direct H-transfer process, see Figure 1). Thus, the required energy barrier of H-shift process is greatly reduced due to the assistance of cocatalyst, and the

rate-determining step of CuBr-catalyzed reaction is changed from the H-transfer process to the intramolecular cyclization step (see Figures 1 and 3).

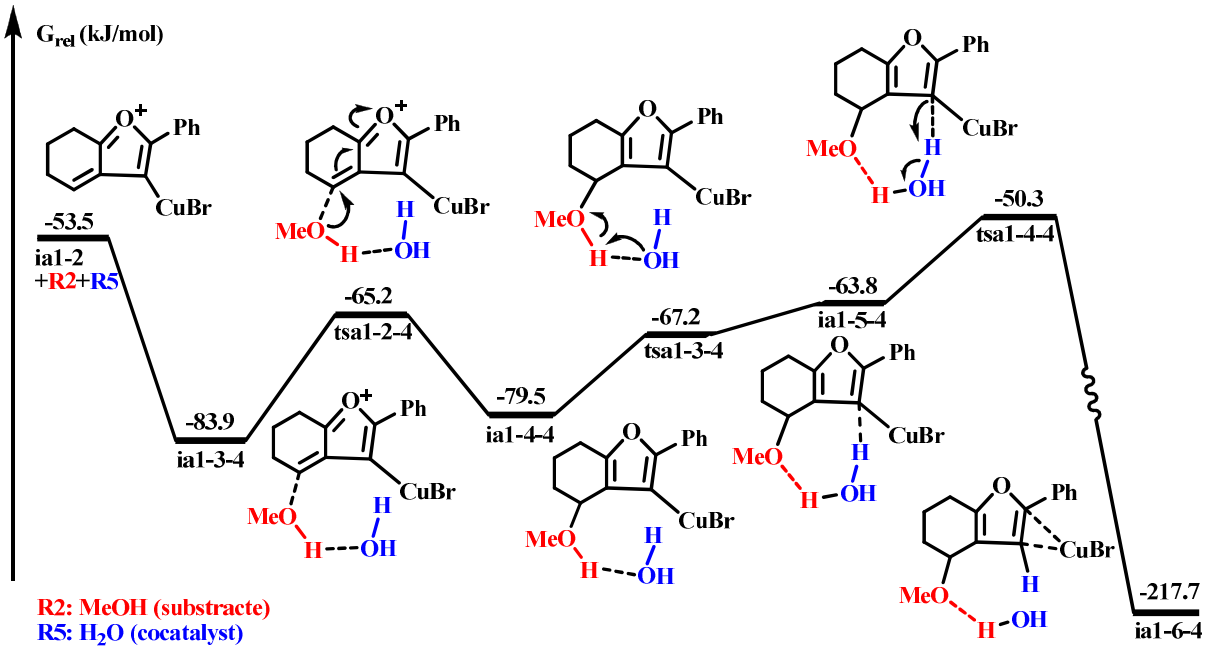

Figure 5. DFT-computed energy profile of the H_2O-assisted process in the CuBr-catalyzed synthesis of highly substituted furans.

Effects of H_2O on the Intermolecular Addition and the H-transfer Process. There is a trace amount of water presented in DMF due to the solvent without drying in experiment. The previous literatures have reported that H_2O also has a significant effect on the catalytic reactions.[9a, 26b, 28] The effect of H_2O, based on the above reasons, is further considered in our present study. The calculated energy profile for H_2O-assisted process is showed in Figure 5, and the geometries of involving intermediates and transition states are collected in Figure 6. Figure 5 shows that the H_2O-assisted process includes an intermolecular nucleophilic addition, a protonation of H_2O and a deprotonation of H_2O-H^+, which is similar to the MeOH-assisted case (see Figure 3). Noteworthy, in the protonation of H_2O (from ia1-4-4 to ia1-5-4), the relative energy of transition state tsa1-3-4 is -67.2 kJ/mol relative to the reaction entrance, which lies 3.4 kJ/mol lower than that of the intermediate

ia1-5-4 (-63.8 kJ/mol). This situation seems to be unreasonable. The IRC calculation of tsa1-3-4 is performed to verify its reliability, as indicated in Figure S27 of the Supporting Information. Calculated result shows that tsa1-3-4 unambiguously connects with ia1-4-4 and ia1-5-4. Moreover,

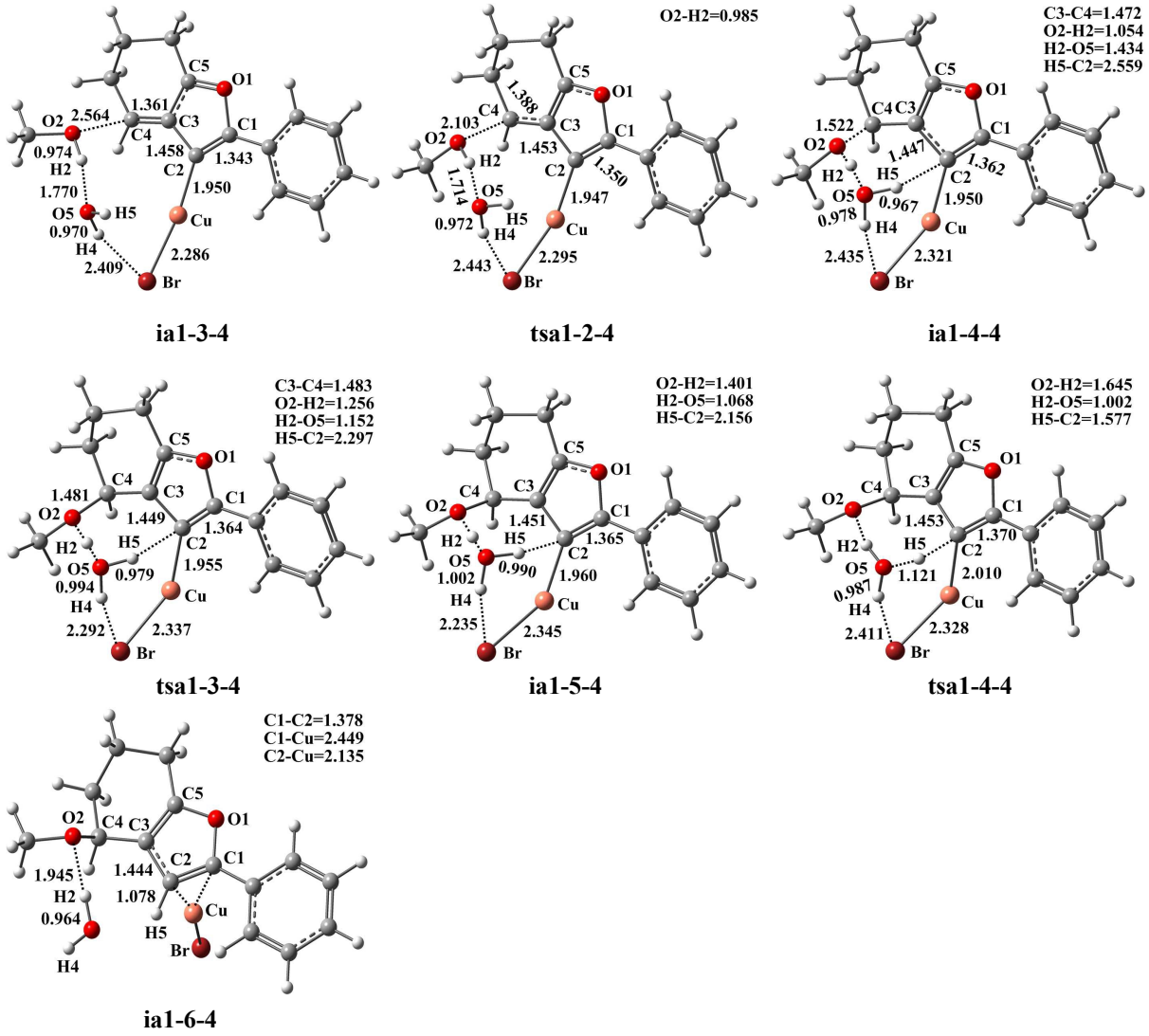

Figure 6. Optimized structures of H_2O-assisted intermolecular addition and stepwise H-transfer process in the CuBr-catalyzed synthesis of highly substituted furans (selected structural parameters are listed (bond lengths in Å)).

the reliability of tsa1-3-4 is also confirmed by animation of its vibrations. In the present H_2O-assisted strategy, H_2O plays similar roles as DMF and MeOH because of its Lewis base character. Due to the assistance of H_2O, the required energy barrier of H-shift process is reduced

from 96.0 to 33.6 kJ/mol (see Figures 5 vs 1). This means that H_2O has a positive effect on the H-transfer process.

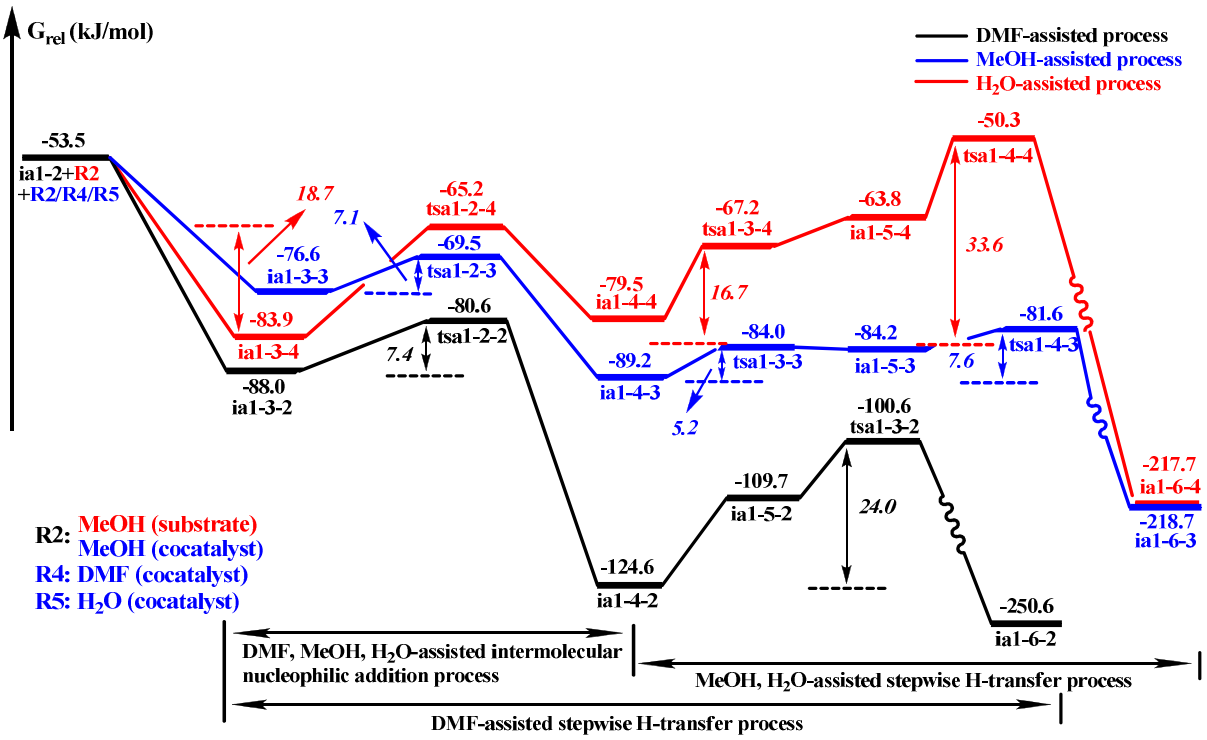

Figure 7. Comparison of DMF, MeOH and H_2O catalytic abilities for the intermolecular nucleophilic addition and the two-step H-transfer process.

Selection of Optimal Catalytic Route. As described in Figure 7, the DMF-assisted route locates below the MeOH- and H_2O-assisted ones. On the one hand, the stabilization energy of ia1-3-2 is higher than that of ia1-3-3 and ia1-3-4 (88.0 vs 78.6 and 83.9 kJ/mol). On the other hand, ia1-4-2 has a lower relative energy than ia1-4-3 and ia1-4-4 (-124.6 vs -89.2 and -79.5 kJ/mol). Based on the above analysis and comparison, it is easy to find that DMF-assisted pathway is the optimal catalytic route for the synthesis of highly substituted furans. Furthermore, DMF as the solvent has a very high concentration in the reaction. The effects of concentration have been considered by the previous literatures.[9c, 29] Thus, the promotion of DMF is more superior to MeOH and H_2O for the present reaction. In optimal catalytic route, there are three elementary reactions including the intramolecular cyclization, the protonation of DMF (the intermolecular nucleophilic addition) and

the deprotonation of DMF-H^+, as illustrated in Figure 8. Their energy barriers are 57.6, 7.4 and 24.0 kJ/mol. Clearly, the rate-determining step is the intramolecular cyclization reaction, and the rate-determining energy barrier is 57.6 kJ/mol.

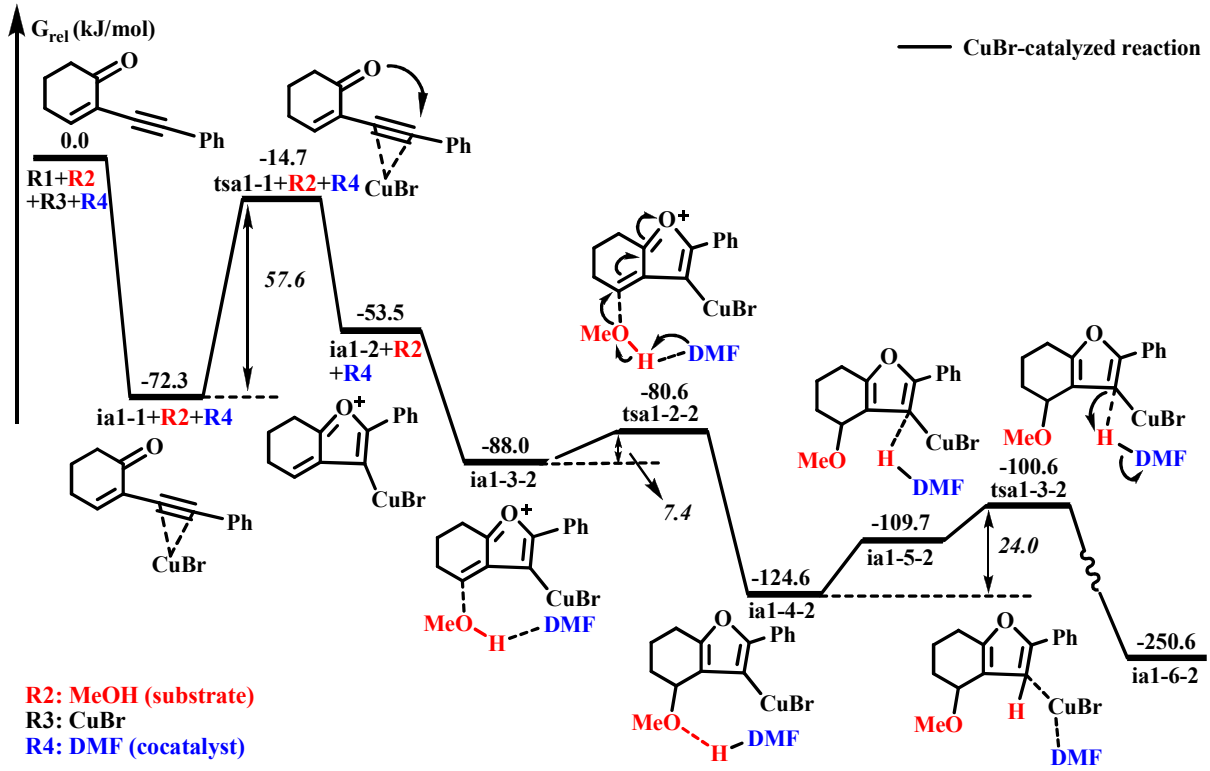

Figure 8. DFT-computed energy profile for the CuBr-catalyzed synthesis of highly substituted furans with the participation of DMF.

3.2. Function of Metal Catalyst CuBr. Yamamoto and his co-workers found that the furans P cannot be obtained in the absence of metal catalyst CuBr. The experimental phenomenon can be explained by the loose scan profile. This method using the loose scan to explain the experimental results has been adopted successfully in the previous theoretical calculations.[30] Loose scan profile of Figure 9 shows that the energy curve is sharp rising in energy with the formation of O1-C1 bond from R1 to in1. It is clear that the intramolecular cyclization reaction between O1 and C1 cannot be carried out without the participation of metal catalyst CuBr. Thus, CuBr is essential for the

cyclization reaction.

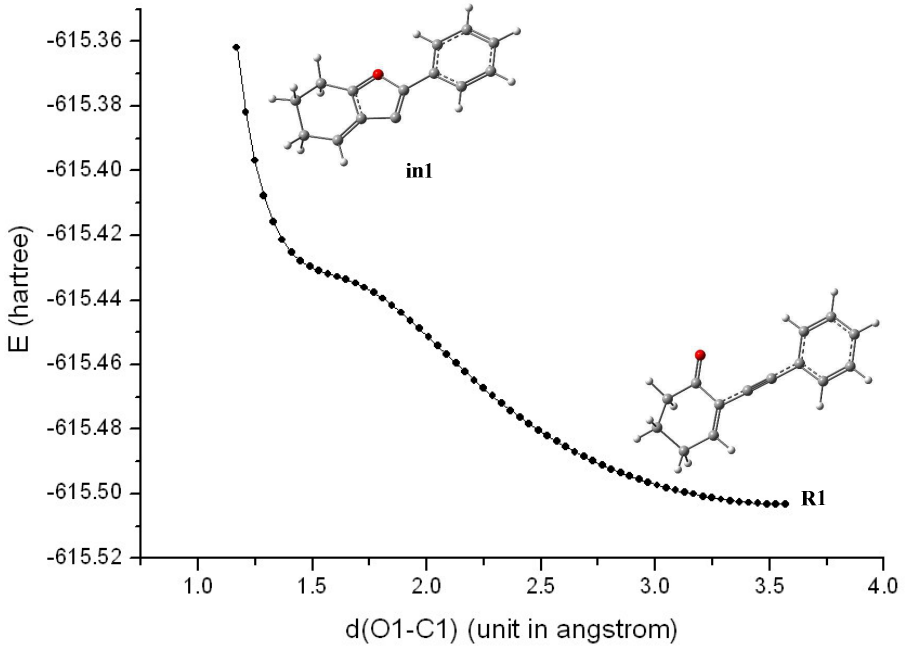

Figure 9. Loose scan profile from R1 to in1 along formation of the O1-C1 bond (from 3.568 to 1.208 Å)

3.3. Effect of Metallic Valence State of Copper. In the experiments[11], the furans P was obtained with a moderate yield (85%), meaning that the yield can be further improved. Our calculations indicate that the intramolecular cyclization reaction is the rate-determining step of the CuBr-catalyzed reaction (see Figure 8). In our previous study,[16d] we have found that the high valence state Cu(II) salts have a strong catalytic ability for the intramolecular cyclization compared with the low valence state Cu(I) salts. Inspired by our research, one inference is that an excellent yield of desired produces P can be got using $CuBr_2$ as the catalyst. In order to confirm our speculation, the mechanism of $CuBr_2$-catalyzed synthesis of furans from 2-(1-Alkynyl)-2-alken-1-ones in DMF medium is investigated in detail. The potential energy surface of optimal path is showed in Figure 10, and the corresponding geometric structures are collected in Figure S11 of the Supporting Information. Similar to the CuBr-catalyzed reaction with DMF as the cocatalyst (see Figure 8), the $CuBr_2$-catalyzed reaction also includes three main

processes, an intramolecular cyclization, a protonation of DMF (DMF-assisted intermolecular addition) and a deprotonation of DMF-H^+. Their energy barriers are 27.3, 5.4 and 50.2 kJ/mol, respectively. The energy barrier of intramolecular cyclization is significantly reduced (27.3 vs 57.6 kJ/mol) when CuBr is substituted with $CuBr_2$ as the metal catalyst. For this reason, the rate-determining step of $CuBr_2$-catalyzed reaction is changed to the deprotonation of DMF-H^+ process (from ia2-4-2 to ia2-6-2). The rate-determining energy barrier is 50.2 kJ/mol, which is 7.4 kJ/mol lower than that of CuBr-catalyzed reaction (50.2 vs 57.6 kJ/mol). Clearly, the reaction can be further accelerated with the use of $CuBr_2$. Therefore, the high valence state of Cu is more suitable than its low valence state for the synthesis of furans base on 2-(1-Alkynyl)-2-alken-1-ones in DMF medium. In addition, we try our best to explore the accelerating effect of Cl ligand on this reaction, but we failed.

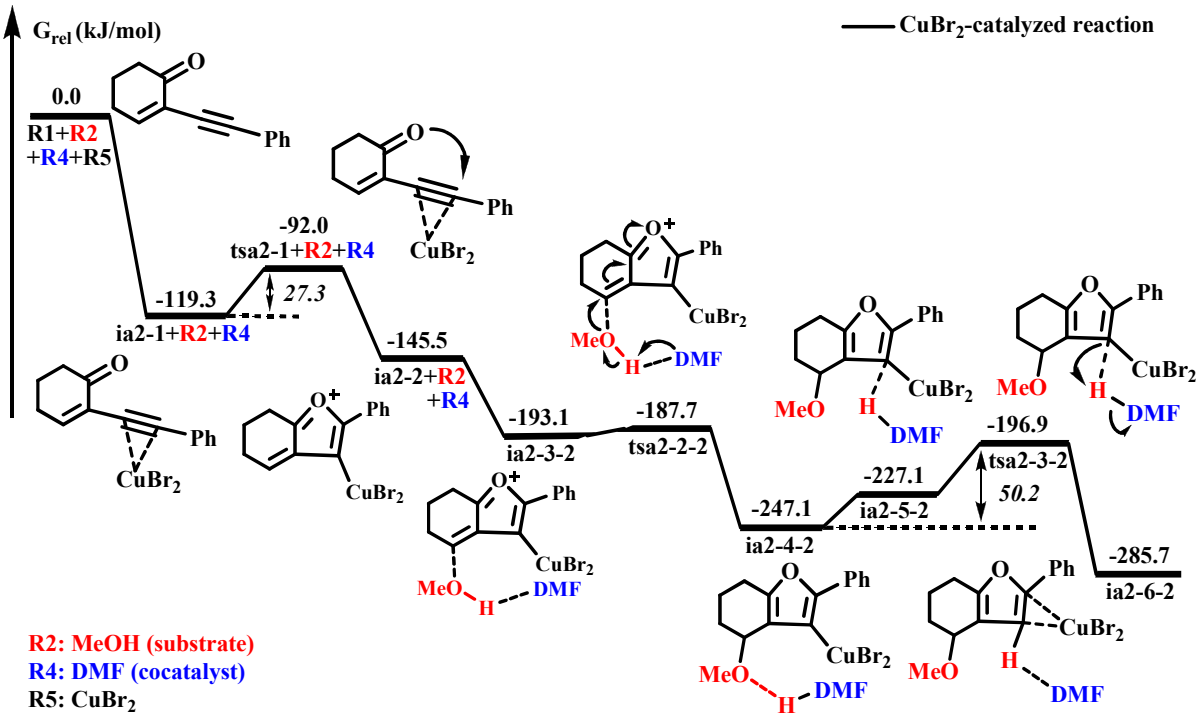

Figure 10. Optimal energy profile for the $CuBr_2$-catalyzed synthesis of highly substituted furans with the participation of DMF.

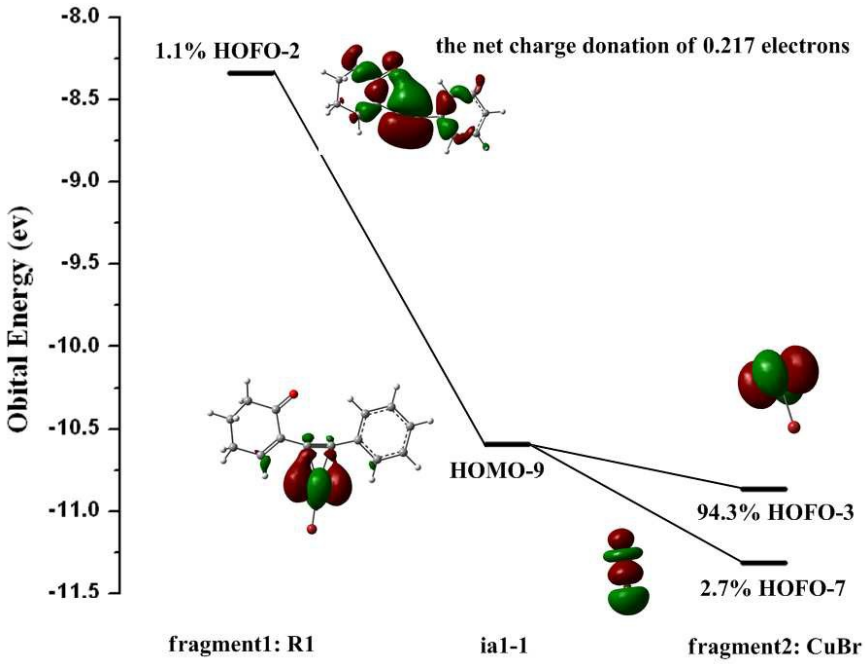

Figure 11. The orbital interaction diagram illustrating the coupling of the R1 and CuBr fragments in ia1-1 complex (the AOMix-CDA calculation at the BHandHLYP/6-31G* level; the net charge donation, is 0.217 electrons from fragment 1 to fragment 2).

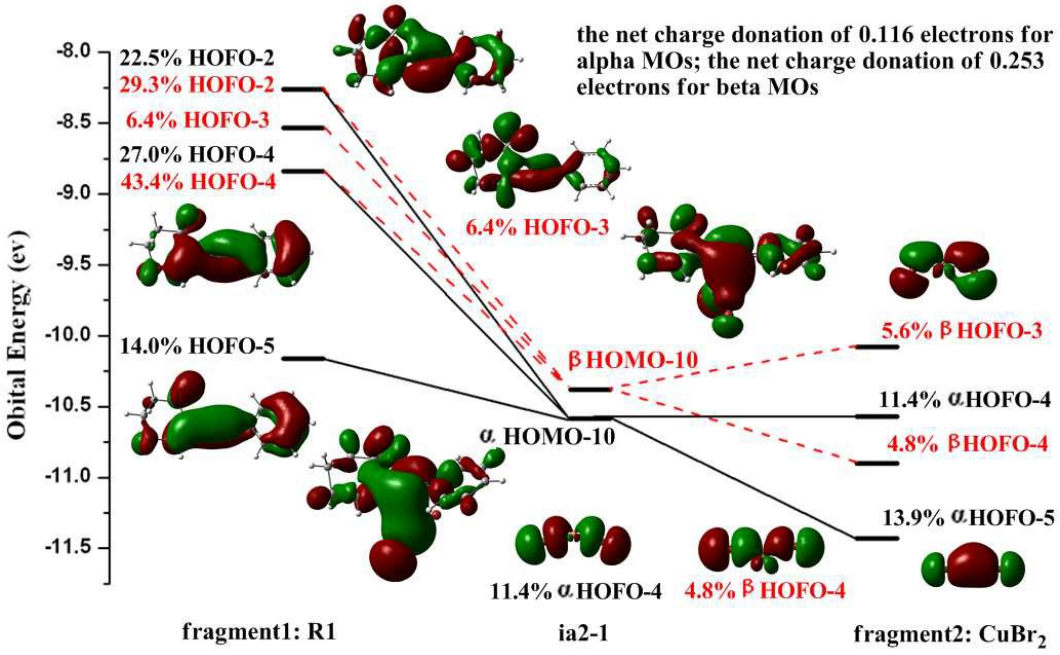

Figure 12. α, β-Spin orbital interaction diagram illustrating the coupling of the R1 and $CuBr_2$ fragments in ia2-1 complex (the AOMix-CDA calculation at the BHandHLYP/6-31G* level; α, β-MOs are shown in black and red respectively; the net charge donation, including the net charge donation of 0.116 electrons for alpha MOs and the charge donation of 0.253 electrons for beta MOs, is 0.369 electrons from fragment 1 to fragment 2)

How to understand the difference of CuBr and $CuBr_2$ in catalytic ability for the intramolecular cyclization reaction? We choose the complexes ia1-1 and ia2-1 as a research system because their electronic structures would affect the intramolecular cyclization between O2 and C4. As shown in Figures 11 and 12, the electronic interaction of substrate R1 (fragment 1) and metal catalyst (CuBr or $CuBr_2$, fragment 2) in ia1-1 and ia2-1 is calculated by the AOMix-CDA program (based on the BHandHLYP/6-31G* results, α and β denote the alpha and beta molecular orbitals (MOs) of ia2-1). In the CuBr-catalyzed reaction, the occupied molecular orbital HOMO-9 of ia1-1 is related with the C1-Cu and C2-Cu coordination bonds. From the results of molecular orbital fragment analyses, HOMO-9 is composed of 1.1% HOFO-2 (the HOMO-2 of fragment orbitals) of R1 and 94.3% HOFO-3 and 2.7% HOFO-7 of fragment 2 (CuBr). Obviously, HOMO-9 is mainly constituted by fragment 2. More importantly, the net charge donation including charge donation and electronic polarization contributions is only 0.217 electrons from fragment 1 to fragment 2. Similarly, HOMO-10 of ia2-1 is also related with the two coordination bonds C1-Cu and C2-Cu in the $CuBr_2$-catalyzed reaction. In contrast to the case of ia1-1, the contribution of HOMO-10 depends mainly on fragment 1. Furthermore, the net charge donation (including the charge donation of 0.116 electrons for alpha MOs and the charge donation of 0.253 electrons for beta MOs) is beyond 0.369 electrons from fragment 1 to fragment 2. According to the above analysis of ia1-1 and ia2-1, the coordination capacity of Cu(II) with C1-C2 triple bond of R1 is stronger than that of Cu(I) with C1-C2 bond (0.217 in ia1-1 vs 0.369 in ia2-1 for the net charge donation from fragment 1 to fragment 2). This is just the crucial reason landing to the difference of CuBr and $CuBr_2$ in catalytic capability for the intramolecular cyclization reaction. Moreover, the orbital interaction diagram of tsa1-1 vs tsa2-1 can give us a similar explanation. This contrast is showed in Figures S14 and S15 of the Supporting Information. Besides, this fact can also be obtained by comparing the stabilization

energies of ia1-1 and ia2-1 relative to the reaction entrance (72.3 vs 119.3 kJ/mol), as indicated in Figures 8 and 10. Of course, this conclusion needs to be proven in our future work.

4 Conclusions

Here, the influence of solvent DMF, substrate MeOH, trace H_2O and valence state of Cu is explored based on the CuBr-catalyzed synthesis of highly substituted furans from 2-(1-alkynyl)-2-alken-1-ones using DFT method at BHandHLYP/6-31G* (LanL2DZ for Cu) level. Calculated results indicate that DMF-assisted strategy for the CuBr-catalyzed synthesis of highly substituted furans is more favorable. DMF can reduce the reaction barrier of the intermolecular nucleophilic addition as a hydrogen-bond acceptor. What's more, the 1.4-trasfer process is changed to the DMF-assisted stepwise H-transfer process due to it's assistance. In this case, DMF acts as a proton shuttle to assist H migration from MeOH to the carbon atom. In addition, we find that MeOH and H_2O also play the similar role as DMF in the intermolecular nucleophilic addition and the H-transfer process. Finally, our calculations predict that the high valence state of Cu would further promote the reaction and increase the reaction yield relative to its low valence state. These interesting findings and insights are valuable for the understanding of the catalytic synthesis of highly substituted furans using transition metal as the catalyst, and they are expected to help us design other new reactions for the metal-catalyzed reaction applications.

Acknowledgments

We acknowledge generous financial support from "the Fundamental Research Funds for the Central Universities (grant no. XDJK2013A008) ".

Supporting Information: DFT-computed energy profiles of all potential reaction pathways, optimized geometries of all involving species, intrinsic reaction coordinate of some key transition states, and so on.

References

1. (a) X.-L. Hou, Z. Yang and H. N. Wong, *Prog. Heterocycl. Chem.,* 2002, **14**, 139-179;
(b) R. C. Brown, *Angew. Chem. Int. Ed.,* 2005, **44**, 850-852;
(c) X. L. Hou, H. Y. Cheung, T. Y. Hon, P. L. Kwan, T. H. Lo, S. Y. Tong and H. N. Wong, *Tetrahedron,* 1998, **54**, 1955-2020;
(d) S. F. Kirsch, *Org. Biomol. Chem.,* 2006, **4**, 2076-2080;
(e) B. Keay, *Chem. Soc. Rev.,* 1999, **28**, 209-215.
2. (a) P. A. Jacobi, K. M. Touchette and H. G. Selnick, *J. Org. Chem.,* 1992, **57**, 6305-6313;
(b) S. P. Tanis, E. D. Robinson, M. C. McMills and W. Watt, *J. Am. Chem. Soc.,* 1992, **114**, 8349-8362;
(c) S. F. Martin and P. W. Zinke, *J. Org. Chem.,* 1991, **56**, 6600-6606;
(d) L. A. Paquette, A. M. Doherty and C. M. Rayner, *J. Am. Chem. Soc.,* 1992, **114**, 3910-3926;
(e) L. A. Paquette and P. C. Astles, *J. Org. Chem.,* 1993, **58**, 165-169.
3. (a) L. Knorr, *Ber. Dtsch. Chem. Ges.,* 1884, **17**, 2863-2870;
(b) C. Paal, *Ber. Dtsch.Chem. Ges.,* 1884, **17**, 2756-2767.
4. (a) D. Schmidt, C. C. Malakar and U. Beifuss, *Org. Lett.,* 2014, **16**, 4862-4865;
(b) D. Nitsch and T. Bach, *J. Org. Chem.,* 2014, **79**, 6372-6379;
(c) J. Barluenga, L. Riesgo, R. Vicente, L. A. Lopez and M. Tomas, *J. Am. Chem. Soc.,* 2008, **130**, 13528-13529;
(d) M. Miao, X. Xu, L. Xu and H. Ren, *Eur. J. Org. Chem.,* 2014, 5896-5900;
(e) T. Wang, S. Shi, M. Rudolph and A. S. K. Hashmi, *Adv. Synth. Catal.,* 2014, **356**, 2337-2342;
(f) Z.-W. Chen, M.-T. Luo, D.-N. Ye, Z.-G. Zhou, M. Ye and L.-X. Liu, *Synth. Commun.,* 2014, **44**, 1825-1831;
(g) T. Wang, L. Huang, S. Shi, M. Rudolph and A. S. K. Hashmi, *Chem. -Eur. J.,* 2014, **20**, 14868-14871;
(h) Y. Xiao and J. Zhang, *Angew. Chem. Int. Ed.,* 2008, **47**, 1903-1906;
(i) Y. Liu, F. Song, Z. Song, M. Liu and B. Yan, *Org. Lett.,* 2005, **7**, 5409-5412;
(j) M. H. Suhre, M. Reif and S. F. Kirsch, *Org. Lett.,* 2005, **7**, 3925-3927.
5. K.-G. Ji, X.-Z. Shu, J. Chen, S.-C. Zhao, Z.-J. Zheng, X.-Y. Liu and Y.-M. Liang, *Org. Biomol. Chem.,* 2009, **7**, 2501-2505.
6. C.-H. Cho, F. Shi, D.-I. Jung and B. Neuenswander, *ACS Comb. Sci.,* 2012, **14**, 403-414.
7. A. W. Sromek, M. Rubina and V. Gevorgyan, *J. Am. Chem. Soc.,* 2005, **127**, 10500-10501.

8. H. Cao, H. Zhan, J. Cen, J. Lin, Y. Lin, Q. Zhu, M. Fu and H. Jiang, *Org. Lett,*. 2013, **15**, 1080-1083.

9. (a) H. Jiang, W. Zeng, Y. Li, W. Wu, L. Huang and W. Fu, *J. Org. Chem.,* 2012, **77**, 5179-5183;

(b) L.-B. Zhao, Z.-H. Guan, Y. Han, Y.-X. Xie, S. He and Y.-M. Liang, *J. Org. Chem.,* 2007, **72**, 10276-10278;

(c) M. Ghosh, S. Mishra and A. Hajra, *J. Org. Chem.,* 2015. **80**, 5364-5368;

(d) C. He, S. Guo, J. Ke, J. Hao, H. Xu, H. Chen and A. Lei, *J. Am. Chem. Soc.,* 2012, **134**, 5766-5769.

10. A. Blanc, K. Tenbrink, J.-M. Weibel and P. Pale, *J. Org. Chem.,* 2009, **74**, 4360-4363.

11. N. T. Patil, H. Wu and Y. Yamamoto, *J. Org. Chem*., 2005, **70**, 4531-4534.

12. N. T. Patil and Y. Yamamoto, *J. Org. Chem.,* 2004, **69**, 5139-5142.

13. M. J. Frisch, G. W. Trucks, H. B. Schlegel, G. E. Scuseria, M. A. Robb, J. R. Cheeseman, G. Scalmani, V. Barone, B. Mennucci, G. A. Petersson, H. Nakatsuji, M. Caricato, X. Li, H. P. Hratchian, A. F. Izmaylov, J. Bloino, G. Zheng, J. L. Sonnenberg, M. Hada, M. Ehara, K. Toyota, R. Fukuda, J. Hasegawa, M. Ishida, T. Nakajima, Y. Honda, O. Kitao, H. Nakai, T. Vreven, J. A. Jr. Montgomery, J. E. Peralta, F. Ogliaro, M. Bearpark, J. J. Heyd, E. Brothers, K. N. Kudin, V. N. Staroverov, R. Kobayashi, J. Normand, K. Raghavachari, A. Rendell, J. C. Burant, S. S. Iyengar, J. Tomasi, M. Cossi, N. Rega, J. M. Millam, M. Klene, J. E. Knox, J. B. Cross, V. Bakken, C. Adamo, J. Jaramillo, R. Gomperts, R. E. Stratmann, O. Yazyev, A. J. Austin, R. Cammi, C. Pomelli, J. W. Ochterski, R. L. Martin, K. Morokuma, V. G. Zakrzewski, G. A. Voth, P. Salvador, J. J. Dannenberg, S. Dapprich, A. D. Daniels, O. Farkas, J. B. Foresman, J. V. Ortiz, J. Cioslowski and D. J. Fox, Gaussian 09, Revision A.02; Gaussian, Inc.: Wallingford, CT, 2009.

14. R. G. Parr and R. G. P. W.Yang, *Density-functional theory of atoms and molecules*; Oxford university press: New York, 1989.

15. (a) A. D. Becke, *J. Chem. Phys.,* 1993, **98**, 5648-5652;

(b) C. Lee, W. Yang and R. G. Parr, *Phys. Rev. B,* 1988, **37**, 785-789.

16. (a) R. Fang, L. Yang and Y. Wang, *Org. Biomol. Chem.,* 2011, **9**, 2760-2770;

(b) R. Fang, C.-Y. Su, C. Zhao and D. L. Phillips, *Organometallics,* 2009, **28**, 741-748;

(c) L. Yang, R. Fang and Y. Wang, *Comput. Theor. Chem.,* 2011, **965**, 180-185;

(d) B. Yuan, R. He, W. Shen, C. Huang and M. Li, *J. Org. Chem.,* 2015, **80**, 6553-6563.

17. (a) V. A. Rassolov, M. A. Ratner, J. A. Pople, P. C. Redfern and L. A. Curtiss, *J. Comput. Chem.,* 2001, **22**, 976-984;

(b) V. A. Rassolov, J. A. Pople, M. A. Ratner and T. L. Windus, *J. Chem. Phys*., 1998, **109**, 1223-1229;

(c) W. J. Hehre, R. Ditchfield and J. A. Pople, *J. Chem. Phys.,* 1972, **56**, 2257-2261.

18. P. J. Hay and W. R.Wadt, *J. Chem. Phys.,* 1985, **82**, 299-310.

19. (a) T. Yang, S. Nagase, T. Akasaka, J. M. Poblet, K. Houk, M. Ehara and X. Zhao, *J. Am. Chem. Soc.,* 2015. **137**, 6820-6828;

(b) B. F. Straub, *Chem. Commun.,* 2004, 1726-1728;

(c) R.-X. Zhu, D.-J. Zhang, J.-X. Guo, J.-L. Mu, C.-G. Duan and C.-B. Liu, *J. Phys. Chem. A,* 2010, **114**, 4689-4696;

(d) Y. Xia, A. S. Dudnik, V. Gevorgyan and Y. Li, *J. Am. Chem. Soc.,* 2008, **130**, 6940-6941.

20. (a) C. Gonzalez and H. B. Schlegel, *J. Chem. Phys.,* 1989, **90**, 2154-2161;

(b) C. Gonzalez and H. B.Schlegel, *J. Phys. Chem.,* 1990, **94**, 5523-5527.

21. (a) S. Gorelsky, *AOMix: Program for molecular orbital analysis*; York University: Toronto (http://www.sg-chem.net);

(b) S. Gorelsky and A. Lever, *J. Organomet. Chem.,* 2001, **635**, 187-196.

22. (a) G. Rauhut, T. Clark and T. Steinke, *J. Am. Chem. Soc.,* 1993, **115**, 9174-9181;

(b) M. W. Wong, K. B. Wiberg and M. J. Frisch, *J. Am. Chem. Soc.,* 1992, **114**, 1645-1652.

23. (a) S. Miertus and J. Tomasi, *Chem. Phys.,* 1982, **65**, 239-245;

(b) M. Cossi, G. Scalmani, N. Rega and V. Barone, *J. Chem. Phys.,* 2002, **117**, 43-54;

(c) T. Mineva, N. Russo and E. Sicilia, *J. Comput. Chem.,* 1998, **19**, 290-299.

24. (a) M. Dell'Acqua, B. Castano, C. Cecchini, T. Pedrazzini, V. Pirovano, E. Rossi, A. Caselli and G. Abbiati, *J. Org. Chem.,* 2014, **79**, 3494-3505;

(b) T. Godet, C. Vaxelaire, C. Michel, A. Milet and P. Belmont, *Chem. -Eur. J.,* 2007, **13**, 5632-5641.

25. Y. X. Liu, D. J. Zhang and S. W. Bi, *J. Phys. Chem.,* 2010, **114**, 12893-12899.

26. (a) X. Zhang and K. Houk, *J. Org. Chem.,* 2005, **70**, 9712-9716;

(b) F.-Q. Shi, X. Li, Y. Xia, L. Zhang and Z.-X. Yu, *J. Am. Chem. Soc.,* 2007, **129**, 15503-15512;

(c) D. Roy, C. Patel and R. B. Sunoj, *J. Org. Chem.,* 2009, **74**, 6936-6943;

(d) P. Verma, P. A. Patni and R. B. Sunoj, *J. Org. Chem.,* 2011, **76**, 5606-5613;

(e) I. Nakamura, N. Shiraiwa, R. Kanazawa and M. Terada, *Org. Lett.,* 2010, **12**, 4198-4200.

27. (a) T. C. Bruice and P. Y. Bruice, *J. Am. Chem. Soc.,* 2005, **127**, 12478-12479;

(b) V. L. Schramm, *Chem. Rev.,* 2006, **106**, 3029-3030;

(c) J. Gao, S. Ma, D. T. Major, K. Nam, J. Pu and D. G. Truhlar, *Chem. Rev.,* 2006, **106**, 3188-3209;

(d) S. W. Ragsdale, *Chem. Rev.,* 2006, **106**, 3317-3337;

(e) X. Zhang and K. Houk, *Acc. Chem. Res.,* 2005, **38**, 379-385.

28. (a) L. Zhang and S. Wang, *J. Am. Chem. Soc.,* 2006, **128**, 1442-1443.

(b) Y. Xia, Y. Liang, Y. Chen, M. Wang, L. Jiao, F. Huang, S. Liu, Y. Li and Z.-X. Yu**,** *J. Am. Chem. Soc.,* 2007, **129**, 3470-3471;

(c) Y. Liang, S. Liu, Y. Xia, Y. Li and Z.-X. Yu, *Chem. -Eur. J.,* 2008, **14**, 4361-4373;

(d) Y. Liang, S. Liu and Z.-X. Yu, *Synlett,* 2009, 905-909.

29. (a) A. K. Sharma and R. B. Sunoj, *Angew. Chem.,* 2010, **122**, 6517-6521;

(b) K. Yamashita, Y. Yamamoto and H. Nishiyama, *J. Am. Chem. Soc.,* 2012, **134**, 7660-7663;

(c) F. Liu, X. Ding, L. Zhang, Y. Zhou, L. Zhao, H. Jiang and H. Liu, *J. Org. Chem.,* 2010, **75**, 5810-5820.

30. J. Zhang, W. Shen, L. Li and M. Li, *Organometallics,* 2009, **28**, 3129-3139.

Graphic Abstract

Comparing the catalytic abilities of DMF, MeOH, and H_2O for intermolecular nucleophilic addition and H-transfer process.